



## Article

# Tricetin Reduces Inflammation and Acinar Cell Injury in Cerulein-Induced Acute Pancreatitis: The Role of Oxidative Stress-Induced DNA Damage Signaling

Máté Nagy-Pénzes<sup>1,2,†</sup>, Zoltán Hajnádý<sup>1,2,†</sup>, Zsolt Regdon<sup>1</sup>, Máté Á. Demény<sup>3</sup> , Katalin Kovács<sup>1,3</sup>, Tarek El-Hamoly<sup>1,4</sup>, József Maléth<sup>5,6,7</sup>, Péter Hegyi<sup>5,8,9</sup>, Csaba Hegedűs<sup>1</sup> and László Virág<sup>1,3,\*</sup>

- <sup>1</sup> Department of Medical Chemistry, Faculty of Medicine, University of Debrecen, 4032 Debrecen, Hungary; nagy.mate@med.unideb.hu (M.N.-P.); hajnady.zoltan@med.unideb.hu (Z.H.); regdike1988@gmail.com (Z.R.); kovacs.katalin@med.unideb.hu (K.K.); tahamoly@hotmail.com (T.E.-H.); hcsaba@med.unideb.hu (C.H.)
- <sup>2</sup> Doctoral School of Molecular Medicine, University of Debrecen, 4032 Debrecen, Hungary
- <sup>3</sup> MTA-DE Cell Biology and Signaling Research Group, 4032 Debrecen, Hungary; demenym@med.unideb.hu
- <sup>4</sup> Drug Radiation Research Department, National Centre for Radiation Research and Technology, Egyptian Atomic Energy Authority, Cairo 11787, Egypt
- <sup>5</sup> First Department of Medicine, University of Szeged, 6720 Szeged, Hungary; maleth.jozsef@med.u-szeged.hu (J.M.); hegyi2009@gmail.com (P.H.)
- <sup>6</sup> HAS-USZ Momentum Epithelial Cell Signalling and Secretion Research Group, 6720 Szeged, Hungary
- <sup>7</sup> Department of Public Health, University of Szeged, 6720 Szeged, Hungary
- <sup>8</sup> Institute for Translational Medicine, János Szentágotthai Research Centre, University of Pécs Medical School, 7624 Pécs, Hungary
- <sup>9</sup> Division of Pancreatic Diseases, Heart and Vascular Center, Semmelweis University, 1122 Budapest, Hungary
- \* Correspondence: lvirag@med.unideb.hu
- † These authors contributed equally to this work.



**Citation:** Nagy-Pénzes, M.; Hajnádý, Z.; Regdon, Z.; Demény, M.Á.; Kovács, K.; El-Hamoly, T.; Maléth, J.; Hegyi, P.; Hegedűs, C.; Virág, L. Tricetin Reduces Inflammation and Acinar Cell Injury in Cerulein-Induced Acute Pancreatitis: The Role of Oxidative Stress-Induced DNA Damage Signaling. *Biomedicines* **2022**, *10*, 1371. <https://doi.org/10.3390/biomedicines10061371>

Academic Editors: Marlene Costa and Fátima Paiva-Martins

Received: 7 May 2022

Accepted: 7 June 2022

Published: 10 June 2022

**Publisher's Note:** MDPI stays neutral with regard to jurisdictional claims in published maps and institutional affiliations.



**Copyright:** © 2022 by the authors. Licensee MDPI, Basel, Switzerland. This article is an open access article distributed under the terms and conditions of the Creative Commons Attribution (CC BY) license (<https://creativecommons.org/licenses/by/4.0/>).

**Abstract:** Acute pancreatitis (AP) poses a worldwide challenge due to the growing incidence and its potentially life-threatening course and complications. Specific targeted therapies are not available, prompting the identification of new pathways and novel therapeutic approaches. Flavonoids comprise several groups of biologically active compounds with wide-ranging effects. The flavone compound, tricetin (TCT), has not yet been investigated in detail but sporadic reports indicate diverse biological activities. In the current study, we evaluated the potential protective effects of TCT in AP. TCT (30  $\mu$ M) protected isolated primary murine acinar cells from the cytotoxic effects of cerulein, a cholecystokinin analog peptide. The protective effects of TCT were observed in a general viability assay (calcein ester hydrolysis), in an apoptosis assay (caspase activity), and in necrosis assays (propidium iodide uptake and lactate dehydrogenase release). The effects of TCT were not related to its potential antioxidant effects, as TCT did not protect against H<sub>2</sub>O<sub>2</sub>-induced acinar cell death despite possessing radical scavenging activity. Cerulein-induced expression of IL1 $\beta$ , IL6, and matrix metalloproteinase 2 and activation of nuclear factor- $\kappa$ B (NF $\kappa$ B) were reduced by 30  $\mu$ M TCT. In vivo experiments confirmed the protective effect of TCT in a mouse model of cerulein-induced AP. TCT suppressed edema formation and apoptosis in the pancreas and reduced lipase and amylase levels in the serum. Moreover, TCT inhibited interleukin-1 $\beta$  (IL1 $\beta$ ), interleukin-6 (IL6), and tumor necrosis factor- $\alpha$  (TNF $\alpha$ ) expression in the pancreas and reduced the activation of the oxidative DNA damage sensor enzyme poly(ADP-ribose) polymerase-1 (PARP-1). Our data indicate that TCT can be a potential treatment option for AP.

**Keywords:** acute pancreatitis; tricetin; inflammation; cell death; necrosis; oxidative stress

## 1. Introduction

The pancreas functions as an exocrine and endocrine organ [1]. The secretion of pancreatic juice containing digestive enzymes (e.g., chymotrypsin, trypsin, lipase, amylase, etc.),

protease inhibitors, and bicarbonate into the intestine is termed the exocrine function of the pancreas [2,3]. The endocrine function includes the production of insulin, glucagon, somatostatin, ghrelin, and amylin by cells of the islets of Langerhans [4,5]. Pancreatitis is an autolytic process initiated in the exocrine pancreas. Autoactivation of zymogenic digestive enzymes is typically triggered by binge alcohol consumption or the formation of bile stones blocking the terminal section of the common bile duct (papilla Vateri) through which both the pancreatic juice and the bile are secreted [2]. Hypertriglyceridemia, infections, toxins, drugs, endoscopic retrograde cholangiopancreatography, and surgery are also linked to acute pancreatitis (AP) and about 10% of AP cases are classified as idiopathic [6,7]. The incidence of AP varies between 13 and 45 cases/100,000 people in developing countries [8] and the incidence of AP is increasing in many countries. The severity of AP ranges from mild, spontaneously healing forms to life-threatening severe cases [9].

Although drugs are generally overused in AP [10,11], treatment options for AP are limited and include two-phases of fluid resuscitation [12] and early enteral feeding [13]. Targeted therapies are not available despite extensive efforts to identify molecular targets for AP treatment.

Several novel treatments were identified in preclinical studies; however, translation of these efforts into the clinic was mostly unsuccessful. Therapies that work in preclinical models of AP include, but are not limited to, nonsteroidal anti-inflammatory drugs (e.g., indomethacin, diclofenac, ketorolac) [14], pentoxifylline [15], calcium channel inhibition with CM4620 [16], poly(ADP-ribose) polymerase (PARP) inhibitors [17–19], peptide hormones (e.g., somatostatin, secretin) [20,21], hemin [22], neostigmine [23], and blocking the TNF $\alpha$  receptor with infliximab [24]. Moreover, various dietary supplements and natural products (e.g., glutamine, resveratrol, spilanthol) [25–29] were also effective in preclinical models of AP. Several ongoing clinical trials aim to determine which of these novel therapeutic approaches can be translated to the clinic.

Polyphenols, including compounds of the flavonoid family, have anti-pancreatitis potential [30]. Flavonoids share the 2-phenyl-1,4 benzopyrone structure, known as the flavone backbone. Flavonoids from most subgroups have been evaluated for potential protective effects in AP. For example, genistein (isoflavone) [31], quercetin (flavonol) [32], naringenin (flavanone) [33], apigenin (flavone) [34], dihydromyricetin (flavanonol) [35], luteolin (flavone) [36], and fisetin (flavonol) [37] either suppressed inflammation, prevented acinar cell damage, or both [38,39]. Tricetin (TCT) (Supplementary Figure S1B) is a flavone compound with likely or proven bioactivity in models of neurotoxicity, Parkinson's disease [40], diabetes [41,42], and bacterial infections [43]. Most studies focus on the potential anticancer and anti-metastatic effects of TCT [44–46]. However, the effects of TCT in AP have not been investigated. Data reporting the anti-inflammatory effects of TCT in other types of inflammations are also scarce [47–49]. Therefore, the aim of this study was to determine if TCT has a protective effect in isolated acinar cells and in an animal model of AP. Our data show that TCT is an effective cytoprotective and anti-pancreatitis agent in a cerulein-induced acinar cell injury model.

## 2. Materials and Methods

### 2.1. Isolation and Culture of Pancreatic Acinar Cells

Pancreatic acinar cells were isolated from male and female C57BL/6j mice and prepared by collagenase digestion as previously described [50]. The cells were cultured in a 5% CO<sub>2</sub> incubator at 37 °C. The cells were grown in endotoxin-free high glucose Dulbecco's modified Eagle's medium (Sigma-Aldrich, St. Louis, MO, USA) supplemented with 2.5% fetal bovine serum, 1% penicillin-streptomycin mixture, 0.25 mg/mL of trypsin inhibitor (Sigma-Aldrich, St. Louis, MO, USA), and 25 ng/mL of recombinant human epidermal growth factor (Sigma-Aldrich, St. Louis, MO, USA).

## 2.2. Cell Treatments

Cells were seeded in 96-well tissue culture plates for viability and cytotoxicity assays, 24-well tissue culture plates for immunofluorescence (IF), and 6-well tissue culture plates for reverse transcription quantitative real-time polymerase chain reaction (RT-qPCR) assays, Western blotting, and NFκB p65 binding assays. Surfaces of the plates were coated with laminin (Sigma-Aldrich, St. Louis, MO, USA) 1 h before seeding. Laminin was discarded and plates were washed with PBS and dried. One hour of pretreatment with various concentrations of TCT (Extrasynthese, Genay, France) was followed by treatment with 100 nM cerulein (Sigma-Aldrich, St. Louis, MO, USA) for 24 h. Cerulein and TCT were dissolved in dimethyl sulfoxide (DMSO) (stock solution). DMSO concentrations were below 0.1% (*v/v*) in cell cultures and did not have any effects on the parameters measured.

## 2.3. Radical Scavenging Assay

The ABTS (2,2'-azinobis-3-ethylbenzothiazoline-6-sulfonic acid) assay was used to determine the radical scavenging (antioxidant) effect of TCT using vitamin C (Sigma-Aldrich, St. Louis, MO, USA) as a positive control. ABTS is a chromogenic free radical generated overnight by combining it with potassium persulfate (7.4 mM ABTS (Merck Millipore, Burlington, MA, USA) + 10% 24.5 mM K-persulfate). Antioxidant properties of the compounds were determined by the decolorization of the intense green ABTS radical solution. The ABTS solution was prepared as described [51]. The ABTS solution was diluted with 50 mM Gly-HCl buffer to reach a concentration where the absorbance of the solution was  $A = 1$  (1 cm light path at 405 nm) in a Spark photometer (Tecan Spark, Männedorf, Switzerland). Three-fold serial dilutions of TCT and vitamin C were pipetted into 96-well plates containing the assay solution and after 30 min incubation time, absorbance was measured at 405 nm.

## 2.4. Cell Viability (Calcein-AM Assay)

A calcein-AM (Sigma-Aldrich, St. Louis, MO, USA) stock solution (4 mM in DMSO) was diluted in medium and was added to the cells cultured in 96-well plates (1 μM final concentration). Calcein-AM was also added to blank wells containing no cells but cell-free medium. After 40 min incubation at 37 °C, fluorescence intensity of the wells containing medium with or without cells was determined at 485/535 nm in a Spark plate reader. Viability was calculated and expressed as a percentage of the control cells.

## 2.5. Lactate Dehydrogenase (LDH) Assay

LDH activity was determined with a commercially available Cytoscan LDH-assay kit purchased from G-Biosciences (St. Louis, MO, USA) following the kit's protocol with slight modifications as follows. Briefly, 50 μL of culture medium was transferred from the cells to 96-well half-area microplates and 50 μL of LDH reagent mixture was added to each well. Supernatants of lysed control cells (prepared by the addition of 10% Triton-X in PBS for 10 min) were used as a positive control (100% LDH activity). After 20 min incubation at room temperature, the absorbance was measured at 490 nm in a Spark microplate reader. Cytotoxicity was calculated with the following equation:

$$\text{Relative LDH release (\%)} = 100 \times (\text{OD}_{\text{sample}} - \text{OD}_{\text{control}}) / (\text{OD}_{\text{lysate}} - \text{OD}_{\text{control}})$$

## 2.6. Propidium Iodide (PI) Uptake

Acinar cells were isolated and seeded into CellCarrier Ultra 96-well microplates (Perkin Elmer, Waltham, MA, USA). Cells were treated with TCT and cerulein or hydrogen peroxide for 24 h. Cells were then stained with propidium iodide (2.5 μg/mL) (Sigma-Aldrich, St. Louis, MO, USA) and Hoechst342 (5 μg/mL) (Sigma-Aldrich, St. Louis, MO, USA) for 15 min. Images were analyzed as previously reported [52] with an Opera Phenix High-Content Analysis system (Perkin Elmer, Waltham, MA, USA) using a 40× air

objective and appropriate laser and filter settings in sequential mode to avoid overlapping of the emission spectra.

### 2.7. Caspase Activity Assay

Acinar cells were isolated and seeded into CellCarrier Ultra 96-well microplates (Perkin Elmer, Waltham, MA, USA). Cells were pretreated for 1 h with TCT (30  $\mu$ M) and then treated with cerulein (100 nM). CellEvent Caspase-3/7 Green reagent (5  $\mu$ M; Thermo Fisher Scientific, Waltham, MA, USA) was added and fluorescence of the CellEvent reagent was detected every 3 h for 18 h with an Opera Phenix High-Content Analysis system (Perkin Elmer, Waltham, MA, USA) using a 40 $\times$  air objective and appropriate laser and filter settings. Cells were identified in bright field mode.

### 2.8. RNA Extraction, Reverse Transcription, and qPCR Analysis

Acinar cells were isolated and seeded into 6-well plates. After treatment (or after collection of pancreas tissues from mice), total RNA was isolated from cells/tissues with TRI reagent (Molecular Research Center, Cincinnati, OH, USA) and RNA purity was checked by measuring the A260/280 ratio. RT-qPCR was performed as described previously [52]. Gene expression levels were normalized to the harmonic mean of 36B4 and RPS26, as reference housekeeping genes. Primers used for RT-qPCR are summarized in Table 1.

**Table 1.** Primers used for RT-PCR.

Gene	Forward Primers (5 $\rightarrow$ 3)	Reverse Primers (5 $\rightarrow$ 3)
IL1 $\beta$	CAACCAACAAGTGATATTCTCCATG	GATCCACACTCTCCAGCTGCA
IL6	GAGGATACCACTCCCAACAGACC	AAGTGCATCATCGTTGTTTCATACA
IL10	GGCGCTGTCATCGATTCTC	ATGGCCTTGTAGACACTTTGG
TNF $\alpha$	CATCTTCTCAAATTCGAGTGACAA	TGGGAGTAGACAAGGTACAACCC
TGF $\beta$	CCGCAACAACGCCATCTATG	GTTCCACATGTTGCTCCACAC
IFN $\gamma$	GGAAGTGGCAAAAGGATGGTG	ATGTTGTTGCTGATGGCCTG
CCL5	TGCAGTCGTGTTTGTCACTC	AGAGCAAGCAATGACAGGGA
CXCL10	GATGACGGGCCAGTGAGAAT	CGTGGCAATGATCTCAACAC
MMP2	AACGGTCGGGAATACAGCAG	GTAACAACGCTTCATGGGGG
36B4	GGACCCGAGAAGACCTCCTT	GCACATCACTCAGAATTCATCC
RPS26	CCACAATTCAGACCTGCTG	GGTAATTTTCCTCCGTCCT

### 2.9. NF $\kappa$ B Assay

To investigate the effect of TCT on nuclear translocation and consensus sequence binding of the NF $\kappa$ B p65 subunit, an NF $\kappa$ B p65 Transcription Factor Assay Kit (Abcam, Cambridge, UK) was used according to the manufacturer's instructions. The cells were pretreated with 30  $\mu$ M TCT, or medium for 1 h and were then treated with a combination of 20 ng/mL murine interferon- $\gamma$  (mIFN $\gamma$ ) (Sigma-Aldrich, St. Louis, MO, USA) and 1  $\mu$ g/mL lipopolysaccharide (LPS) (Sigma-Aldrich, St. Louis, MO, USA) or with 1  $\mu$ M phorbol 12-myristate 13-acetate PMA (Sigma-Aldrich, St. Louis, MO, USA) for 1 h. Nuclear fractions were extracted from the cells using the protocol supplied with the kit. To investigate the direct effect of TCT on NF $\kappa$ B DNA binding, TCT (30  $\mu$ M) was added to some nuclear extract samples 1 h before the binding assay. Absorbance was measured at 450 nm and DNA binding capacity of the p65 subunit was expressed as a percentage of the control.

### 2.10. PARP Inhibition Assay

To determine the PARP inhibitory effect of TCT, a PARP Activation Kit (Trevigen, Gaithersburg, Maryland, USA) was used according to the manufacturer's instructions; 3-aminobenzamide (3-AB) was used as a positive PARP inhibitor control. The concentrations of TCT and 3-AB were 10 mM, 1 mM, 300  $\mu$ M, 100  $\mu$ M, 30  $\mu$ M, 10  $\mu$ M, 3  $\mu$ M, 1  $\mu$ M, 0.3  $\mu$ M, 0.1  $\mu$ M, and 0.1 nM.

### 2.11. Immunofluorescent (IF) Staining of Acinar Cells

Acinar cells were isolated and seeded onto 13 mm coverslips (Thermo Fisher Scientific, Waltham, MA, USA). The cells were treated with 250  $\mu$ M hydrogen peroxide (7.5 min) with or without 10–30  $\mu$ M TCT pretreatment (1 h). Coverslips were incubated in methanol for 20 min at  $-20$  °C, washed with phosphate-buffered saline (PBS), and lysed with 10% Triton-X in PBS. After blocking in 1% bovine serum albumin (BSA) in PBS at room temperature, cells were incubated with a mouse monoclonal poly(ADP-ribose) (PAR) specific antibody (purified in-house from the supernatant of the 10H hybridoma; isotype IgG3) overnight at 4 °C. On the following day, cells were incubated with a goat anti-mouse Alexa633-conjugated secondary antibody (Thermo Fisher Scientific, Waltham, MA, USA) (1:1000) and 4',6-diamidino-2-phenylindole (DAPI) (Sigma-Aldrich, St. Louis, MO, USA) (1:2000) at room temperature. The coverslips were viewed with an SP8 Leica confocal microscope. The intensity of the PAR signal was analyzed with ImageJ software.

### 2.12. Western Blot Analysis

Acinar cells were isolated and seeded into 6-well tissue culture plates. The cells were treated with 250  $\mu$ M hydrogen peroxide for 7.5 min with or without 10 and 30  $\mu$ M TCT pretreatment (1 h). Total protein lysates were separated on 8% SDS-PAGE gels at 100 V for 90 min. Proteins were transferred to nitrocellulose membranes. Membranes were blocked with 5% BSA in phosphate buffered saline with Tween<sup>®</sup> 20 (PBST) for 1 h at room temperature. Membranes were incubated with antibodies against PAR (clone 10H; purified in-house) overnight at 4 °C. After washing with Tris buffered saline with Tween<sup>®</sup> 20 (TBST), membranes were incubated with peroxidase-conjugated anti-mouse IgG (1:3000; Cell Signaling, Danvers, MA, USA) and anti- $\beta$ -actin (1:20,000; Santa Cruz Biotechnology, Santa Cruz, CA, USA) antibodies for 2 h at room temperature. Membranes were then washed with PBST and incubated with WestFemto chemiluminescent reagent (Thermo Fisher Scientific, Waltham, MA, USA). Luminescence was detected with a Chemidoc Touch gel documentation system (BioRad Laboratories, Hercules, CA, USA). Signal intensities were quantified using Image Lab software (BioRad). The blot area used for signal quantification was selected to cover the PARylated PARP1 region (ca. 100–180 kDa) and actin signals were used for normalization.

### 2.13. Acute Pancreatitis Model

Animal experiments were approved by the institutional animal welfare committee of University of Debrecen protocol number: 25/2017/DEMÁB. Mice (C57BL/6j, 8–10 weeks old) were bred and maintained at 21–23 °C, 30–60% relative humidity, and a 12 h light/dark cycle. Mice were housed in Eurostandard Type II cages and were fed ad libitum with VRF1 (P) food and water. Acute pancreatitis was induced as previously described [53] with modification as follows. Male mice ( $n = 18$ ) were randomized into three groups: control, cerulein, and cerulein + TCT. Mice in the control group were given saline only. In the cerulein-treated group, AP was induced by eight intraperitoneal injections of cerulein (50  $\mu$ g/kg BW) at hourly intervals. In the cerulein + TCT group, mice received two intraperitoneal injections of TCT (10 mg/kg BW) 12 h and 1 h before the first cerulein injection.

We also tested the in vivo efficacy of TCT in a posttreatment setting. Control ( $n = 5$ ), cerulein-treated ( $n = 6$ ), and cerulein + TCT-treated mice ( $n = 6$ ) received two i.p. injections of TCT (30 mg/kg BW) between the fourth and fifth cerulein injections and 10 mg/kg BW of TCT after the last cerulein injection. We chose TCT doses mainly based on literature data on the effects of flavonoids in the mouse model of AP. The flavonol compound fisetin [37] and the prenylated flavonol glycoside icariin [54] were both administered i.p. and their doses were the same as ours (10 mg/kg). The flavonoid most closely related to TCT luteolin was used in 25–50–100 mg/kg doses in a study [36]. Since a posttreatment is always less effective than a pretreatment, for the posttreatment protocol we chose a higher first dose (30 mg/kg) to quickly reach a potentially therapeutic serum concentration and a low second dose (10 mg/kg) for “maintenance” therapy.

Mice in the control and cerulein groups were given saline (with 0.3% DMSO) instead of TCT. The DMSO contents of the cerulein and TCT solutions were 0.1% and 0.3%, respectively. Mice were sacrificed 10 h after the first cerulein injection in both the pretreatment and posttreatment experiments and blood and pancreas tissues were collected.

#### 2.14. Serum $\alpha$ -Amylase and Lipase Determination

Blood samples were taken by cardiac puncture and were centrifuged at  $5000\times g$  for 10 min at  $4\text{ }^{\circ}\text{C}$ . Serum  $\alpha$ -amylase and lipase activities were measured (using an enzymatic assay kit from Diagnosticum Zrt., Budapest, Hungary) in a kinetic reaction over 20 min according to the manufacturer's instructions using a Spark plate reader at 405 nm ( $\alpha$ -amylase) and 580 nm (lipase). Absorbance was measured every 15 s to generate a kinetic curve. The slope of the curves was related to the slope of the control sample curve.

#### 2.15. Myeloperoxidase Assay

Tissue myeloperoxidase (MPO) activity was measured as an indicator of neutrophil infiltration in the pancreas, as described previously [26] with modifications as follows. Tissue samples were thawed, homogenized in 1 mL of 20 mM phosphate buffer (pH 7.4), and centrifuged at  $13,000\times g$  for 30 min at  $4\text{ }^{\circ}\text{C}$ . The resulting pellet was resuspended in 0.5 mL of 50 mM phosphate buffer (pH 6.0) containing 0.5% hexadecyltrimethylammonium bromide (Sigma-Aldrich, St. Louis, MO, USA). The homogenates were then frozen in liquid nitrogen and thawed on three consecutive occasions before sonication. Total protein concentration was measured with a Direct Detect Spectrometer (Merck Millipore, Burlington, MA, USA). The samples were then centrifuged ( $13,000\times g$  for 30 min at  $4\text{ }^{\circ}\text{C}$ ), and the supernatants were collected for the MPO assay. Supernatants (100  $\mu\text{L}$ ) were mixed with 100  $\mu\text{L}$  substrate solution containing 1.6 mM 3,3',5,5'-tetramethylbenzidine (Sigma Aldrich, St. Louis, MO, USA) and 1 mM hydrogen peroxide. The mixture was incubated at  $37\text{ }^{\circ}\text{C}$  for 90 s, and the reaction was stopped with 200  $\mu\text{L}$  2 M  $\text{H}_2\text{SO}_4$ . The absorbance was measured using a Tecan Spark plate reader at 450 nm and then normalized to total protein content.

#### 2.16. Histology

Pancreatic tissues were collected and fixed in 10% formalin for 48 h. Dehydration, embedding, sectioning, and staining with hematoxylin and eosin were performed according to guidelines in [55]. The TUNEL (terminal deoxynucleotidyl transferase dUTP nick end labeling) assay was performed with a TUNEL Assay Kit—HRP—DAB (Abcam, Cambridge, UK) according to the manufacturer's instructions.

Staining was scored by a pathologist blinded to the experimental design and identity of the samples. A scoring scheme from 0 to 3 for edema, leukocyte infiltration, necrosis, and TUNEL assay was used [56], as presented in Table 2.

**Table 2.** Histologic scoring of tissue sections.

	0	1	2	3
Edema	no edema	interlobular edema	interlobular and moderate intralobular edema	interlobular and severe intralobular edema
Infiltration	absent	low perivascular infiltration	moderate perivascular and low diffuse infiltration	severe diffuse infiltration
Necrosis	none or negligible	observed in one third of the cells	observed in half of the cells	observed in most cells
TUNEL	0–5 average spot number/400 $\times$ field	6–15 average spot number/400 $\times$ field	16–35 average spot number/400 $\times$ field	>5 average spot number/400 $\times$ field

#### 2.17. Immunofluorescent (IF) Detection of PAR Polymers in Tissue Sections

Poly(ADP-ribose) (PAR) polymer was detected by immunofluorescence, as described previously [57]. Sections (5  $\mu\text{m}$ ) of pancreatic tissue were blocked with 1% BSA in PBS for

1 h at room temperature and then incubated with mouse monoclonal poly(ADP ribose) antibody (purified in-house) at 3 µg/mL concentration overnight at 4 °C. The tissues were then incubated with Alexa633-conjugated goat anti-mouse IgG secondary antibody (Thermo Fisher Scientific, Waltham, MA, USA) (1:1000), and DAPI (Sigma-Aldrich, St. Louis, MO, USA) (1:2000) at room temperature. Sections were viewed with a Leica Sp8 Confocal Microscope (Leica, Wetzlar, Germany). The PAR signal was analyzed using ImageJ software. PARylation rates were calculated and expressed as intensity values.

### 2.18. Statistical Analysis

In vitro experiments were repeated at least three times and all values are expressed as mean ± SD. The Kolmogorov-Smirnov test was used to check if continuous variable data displayed normal distribution. All data showed normal distribution. One- or two-way ANOVA followed by a Tukey post hoc test was used for analysis. Discrete variables (scores of micrographs) were analyzed using Fisher's exact test. The value of  $p < 0.05$  was considered significant.

## 3. Results

### 3.1. Tricetin Is Nontoxic to Acinar Cells

Isolated acinar cells are a good cell model for studying the exocrine pancreas. We isolated primary acinar cells from mice and tested the toxicity of TCT. Cell viability was evaluated with calcein assay and plasma membrane injury was assessed with LDH release assay using hydrogen peroxide (1 mM) as a positive control. We found that TCT was non-toxic to primary acinar cells up to a concentration of 30 µM (Supplementary Figure S1). At three times higher concentration (100 µM), TCT had a small but significant toxic effect on acinar cells. This could be observed in both the calcein and LDH release assays (Supplementary Figure S1). Therefore, we chose 30 µM TCT for the subsequent cell-based experiments.

### 3.2. Tricetin Protects Isolated Acinar Cells from Cerulein-Induced but Not from Hydrogen Peroxide-Induced Cell Death

The cholecystokinin analog peptide, cerulein, is used extensively to model overstimulation-induced acinar cell injury both in cell-based experiments and in vivo. At 100 nM concentration, cerulein decreased cell viability of primary acinar cells, as indicated by the calcein assay (Figure 1A).

This effect was also observed in the LDH release assay (Figure 1B). Pretreatment of the cells with 30 µM TCT significantly protected acinar cells from cerulein-induced injury in both assays (Figure 1A,B). Necrotic cell death and cell membrane injury are critical features of AP; thus, we also examined the effects of TCT on propidium iodide (PI) uptake. The effects of cerulein and TCT on PI uptake were consistent with the results of both the LDH release and the calcein assays (Figure 1C). Apoptotic cell death could also be observed in the cerulein-treated cells as indicated by increased caspase activity (Figure 1D,E). Pretreatment of cells with 30 µM TCT significantly reduced caspase activation (Figure 1D). Representative fluorescent images also illustrate reduced caspase activation in TCT-treated acinar cells (Figure 1E).

TCT displayed radical scavenging activity (ABTS radical scavenging assay) similar to that of vitamin C (Supplementary Figure S2A). Therefore, we tested whether this effect translates to cytoprotection from H<sub>2</sub>O<sub>2</sub>-induced cell injury. H<sub>2</sub>O<sub>2</sub> caused a concentration-dependent cytotoxicity (Supplementary Figure S2B–D) but TCT had no effect on H<sub>2</sub>O<sub>2</sub>-induced toxicity. Collectively, these results indicate that TCT interferes with the cerulein-induced acinar cell death pathways (Supplementary Figure S2B–D).

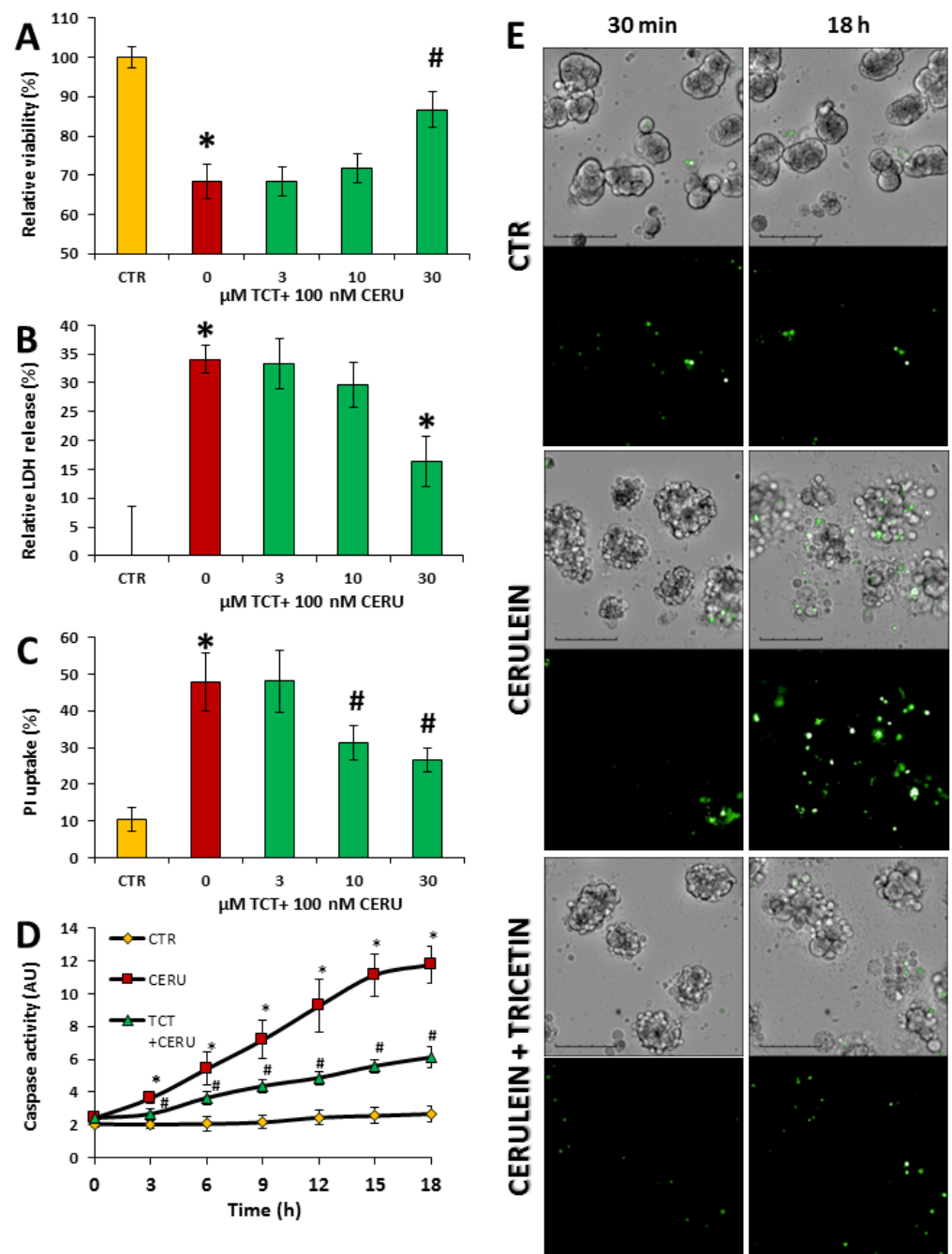


**Figure 1.** Tricetin protects isolated acinar cells from cerulein-induced cell death. Primary acinar cells were pretreated with 0–30  $\mu\text{M}$  tricetin (TCT) for 1 h and then treated with 100 nM cerulein for 24 h. Viability was determined with calcein assays (A), and necrotic cell death was measured by LDH release (B) and propidium iodide (PI) uptake assays (C). Primary acinar cells were pretreated with 30  $\mu\text{M}$  tricetin (TCT) or medium for 1 h and then treated with 100 nM cerulein. Caspase activity was detected every 3 h for 18 h as described in the Materials and Methods section (D). Representative images of caspase activity detection at the first and the last time points are shown (E). (Scale bar is 100  $\mu\text{m}$ ) Error bars represent the SD of three independent measurements. Statistical analysis was performed with one-way ANOVA test followed by Tukey's post hoc test. Stars (\*) indicate significant ( $p < 0.05$ ) difference between cerulein-treated cells versus control. Hashtags (#) indicate significant ( $p < 0.05$ ) cytoprotection by TCT versus the cerulein-treated group.

### 3.3. Cerulein-Induced Expression of Interleukin-1 $\beta$ (IL-1 $\beta$ ), Interleukin-6 (IL6), and Matrix Metalloproteinase-2 (MMP2) Was Attenuated by Tricetin in Primary Pancreatic Acinar Cells

Inflammation contributes to the development of AP. However, AP is unique in the sense that the primary event is cell injury and inflammation develops as a consequence of tissue damage. Nonetheless, suppression of injury-associated inflammation has a beneficial effect on the course of AP. Therefore, the effects of TCT on a set of inflammatory mediators were investigated (Figure 2A).

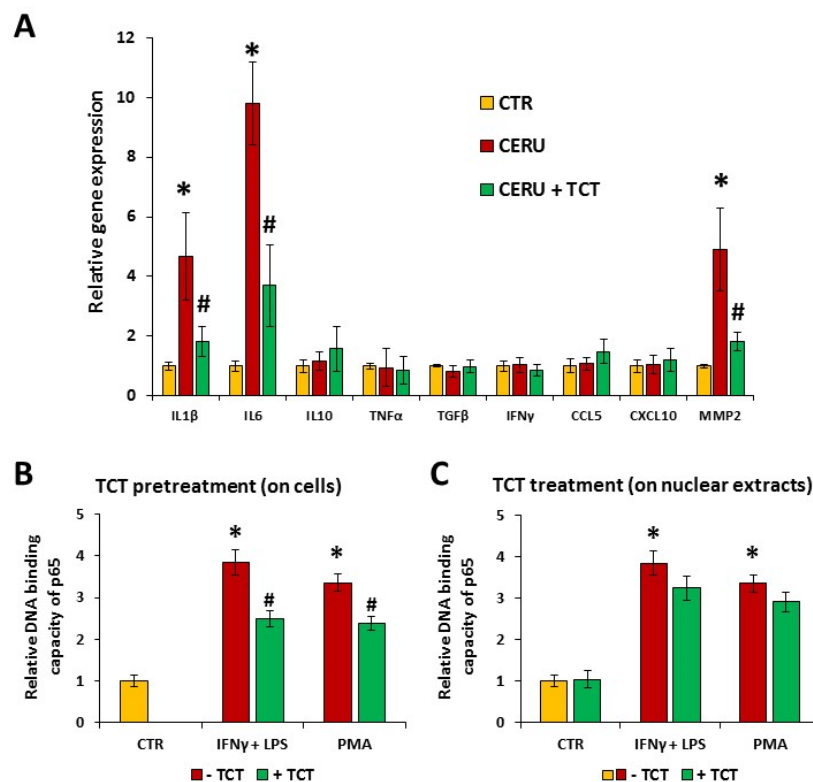


**Figure 2.** Tricetin reduces the expression of IL1 $\beta$ , IL6, and MMP2 genes, and inhibits NF $\kappa$ B activation in primary pancreatic acinar cells. Primary acinar cells were pretreated with 30  $\mu$ M tricetin (TCT) or medium for one hour followed by 100 nM cerulein treatment. After 24 h, mRNA levels were measured with RT-qPCR. Error bars represent the SD of five (or three in the cases of CCL5 and CXCL10) independent experiments. Stars (\*) indicate significant ( $p < 0.05$ ) differences between cerulein-treated cells versus control. Hashtags (#) indicate significantly ( $p < 0.05$ ) reduced gene expression by TCT versus the cerulein-treated group (A). Primary acinar cells were pretreated with 30  $\mu$ M TCT or medium for one hour followed by 20 ng/mL mIFN $\gamma$  + 1  $\mu$ g/mL LPS, or 1  $\mu$ M PMA treatment for one hour. Nuclear fractions were extracted from the cells and were used in NF $\kappa$ B p65 binding assays as described in the Materials and Methods section (B). Part of the nuclear fractions were treated with 30  $\mu$ M TCT to investigate the effect of TCT on the DNA binding of NF $\kappa$ B (C). Statistical analysis was performed with one-way (panel (A)) or two-way (panels (B,C)) ANOVA test followed by Tukey's post hoc test.

Cerulein treatment induced the expression of IL1 $\beta$ , IL6, and MMP2 mRNAs, whereas TNF $\alpha$ , IFN $\gamma$ , TGF $\beta$  (transforming growth factor- $\beta$ ), IL10, CCL5 (chemokine (C-C motif) ligand 5), and CXCL10 (C-X-C motif chemokine ligand 10) expression was not induced by cerulein. Pretreatment of acinar cells with TCT reduced the cerulein-induced expression of IL1 $\beta$ , IL6, and MMP2 (Figure 2A).

### 3.4. Tricetin Inhibits NF $\kappa$ B Signaling

We hypothesized that the effect of TCT on cytokine and MMP2 expression may be due to interference with NF $\kappa$ B signaling. In response to various inflammatory signals,

NF $\kappa$ B is activated, translocates to the nucleus, and mediates the expression of inflammatory mediator genes. The nuclear translocation of NF $\kappa$ B p65 could be observed in acinar cells treated with IFN $\gamma$  + LPS or PMA (Figure 2B,C). TCT (30  $\mu$ M, 1 h) pretreatment significantly decreased nuclear translocation of p65 (Figure 2B). However, addition of TCT to the nuclear extracts had no effect on the DNA binding of p65 subunit (Figure 2C).

### 3.5. Tricetin Inhibits PARP1 and Suppresses H<sub>2</sub>O<sub>2</sub>-Induced Poly(ADP-ribosylation) (PARylation) in Isolated Acinar Cells

Activation of PARP1 contributes to tissue injury and inflammation in acute and chronic pancreatitis [58,59]. Therefore, we investigated whether TCT affected PARylation. In an enzyme activity assay, TCT inhibited PARP activity to a similar extent as the reference compound, 3-aminobenzamide (3-AB) (Figure 3A). The EC<sub>50</sub> for 3-AB was 25  $\mu$ M, and the EC<sub>50</sub> of TCT was 18  $\mu$ M.

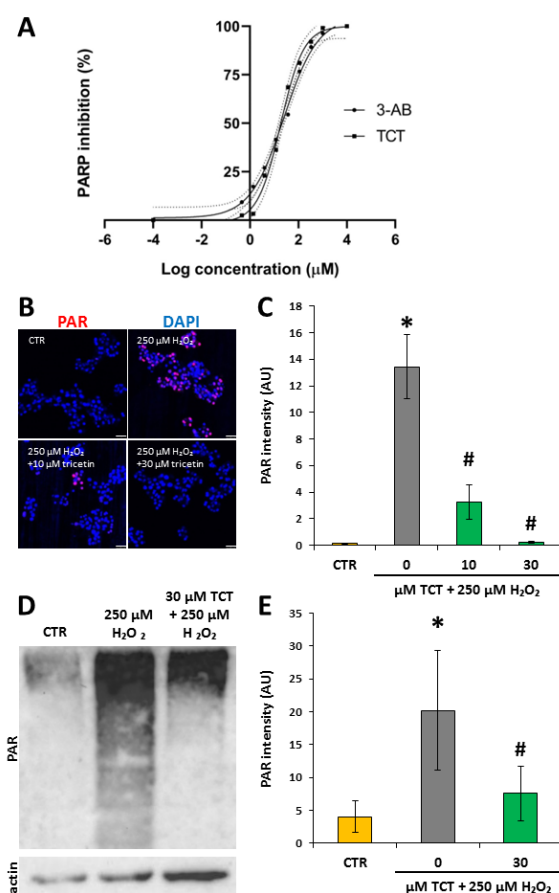


**Figure 3.** Tricetin inhibits PARP in enzyme activity assays and in isolated acinar cells. Tricetin (TCT) inhibits PARP1, as measured with a PARP activation kit (A). Primary acinar cells were pretreated with 10  $\mu$ M or 30  $\mu$ M TCT for one hour and then treated with 250  $\mu$ M hydrogen peroxide for 7.5 min. Immunocytochemical staining of PAR polymer was evaluated with confocal microscopy followed by image analysis with ImageJ software (scale bar 50  $\mu$ m) (B,C). PAR polymer, the product of PARP enzymes, was detected in Western blots and signals were quantitated with ImageLab software and were normalized to actin signal intensities (D,E). Error bars represent the SD of three (IF) or four (WB) independent experiments. Statistical analysis was performed with one-way ANOVA test followed by Tukey's post hoc test. Stars (\*) indicate significant ( $p < 0.05$ ) H<sub>2</sub>O<sub>2</sub>-induced PARylation compared to the control. Hashtags (#) indicate significant ( $p < 0.05$ ) reduction of the PAR signal in TCT-treated samples versus H<sub>2</sub>O<sub>2</sub>-treated cells.

Moreover, hydrogen peroxide-induced PAR synthesis in isolated acinar cells was abolished by 30  $\mu$ M TCT, as indicated by the lack of PAR polymer formation (detected by IF and

Western blotting; Figure 3B–E). Of note, a smear-like appearance of PARylated proteins as seen in Figure 3D is normal because acceptor proteins can be modified with a varying number of negatively charged ADP-ribose units, greatly affecting their electrophoretic mobility.

### 3.6. Tricetin Pretreatment Protects Mice from Cerulein-Induced Acute Pancreatitis

Acute pancreatitis was induced in mice with cerulein, and mice were terminated 3 h after the last cerulein injection (Figure 4A).

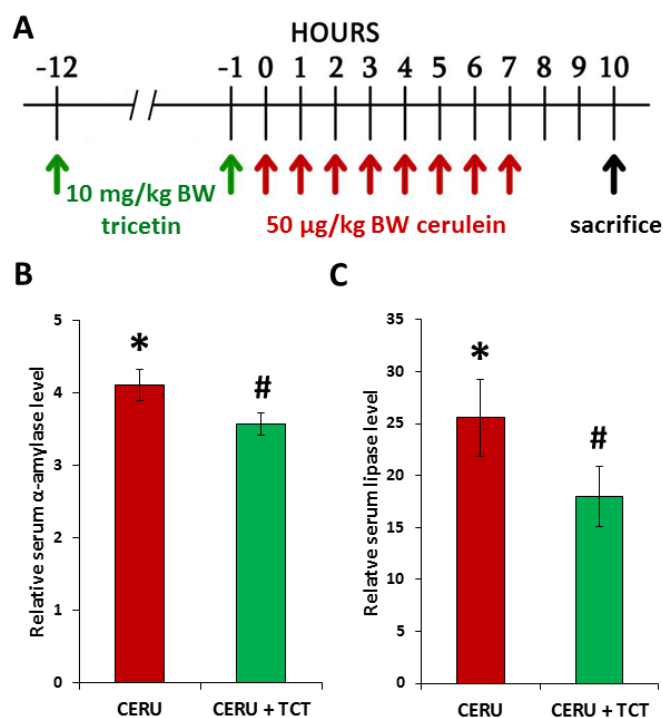


**Figure 4.** Tricetin inhibits tissue injury in acute pancreatitis. Acute pancreatitis was induced in mice with intraperitoneal injections ( $8 \times 50 \mu\text{g/kg BW}$ ) of cerulein at hourly intervals. The animals were sacrificed 10 h after the first cerulein injection. Tricetin (TCT) was applied as a pretreatment ( $2 \times 10 \text{ mg/kg BW}$ ) in i.p. injections, 12 h and 1 h before the first cerulein injection (A). Serum levels of amylase and lipase were measured. Error bars represent SD of six mice. Statistical analysis was performed with one-way ANOVA test followed by Tukey's post hoc test. The cerulein treatment caused significantly ( $* p < 0.05$ ) elevated serum alpha amylase (B) and lipase (C) levels, which were significantly ( $\# p < 0.05$ ) reduced by TCT pretreatment (B,C).

The effects of TCT ( $10 \text{ mg/kg BW}$ ) given at 1 and 12 h before the first cerulein injection were examined. The TCT dose was selected from in vivo studies in which a similar compound fisetin (a flavonol) was investigated [37]. As expected, cerulein caused acinar cell injury indicated by the elevated serum levels of lipase and amylase (Figure 4B). TCT significantly reduced acinar cell injury, as reflected by decreased serum lipase and amylase levels (Figure 4B). Moreover, analysis of H&E-stained sections revealed edema in the pancreas of cerulein-treated mice (Figure 5A). TCT prevented edema formation, neutrophil infiltration, necrosis (Figure 5A), and formation of TUNEL positive cells/apoptotic bodies (Figure 5B), as verified by semiquantitative analysis of the sections (Figure 5C).

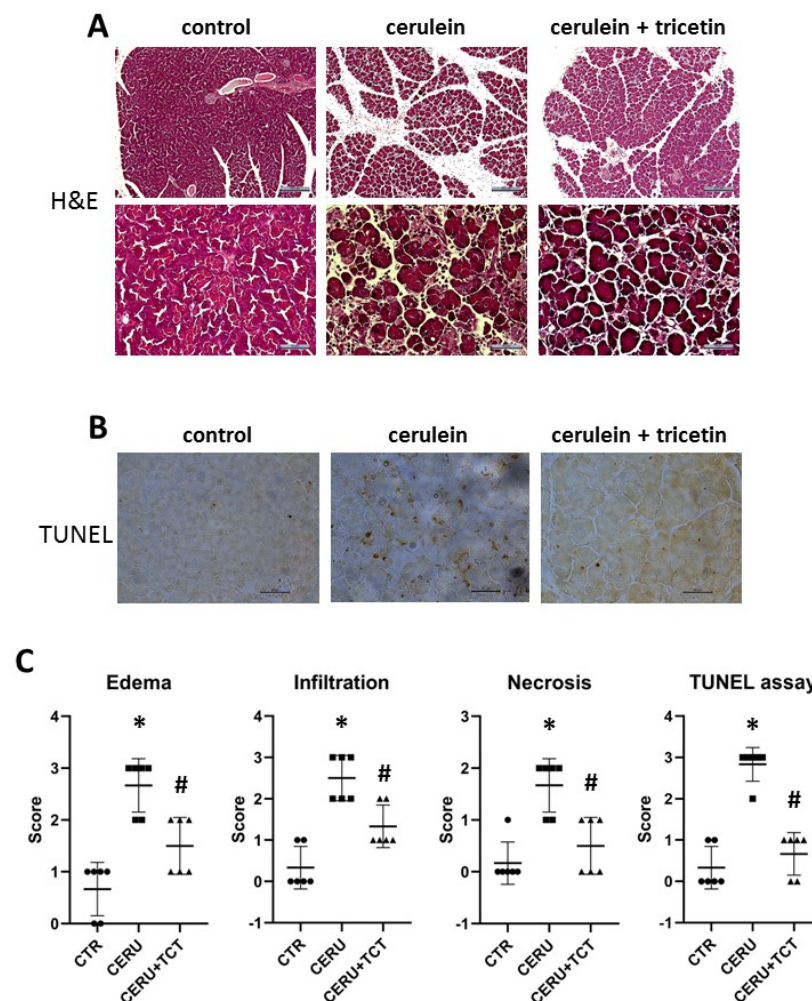


**Figure 5.** Tricetin inhibits tissue injury, edema, apoptosis, and necrosis in acute pancreatitis. Micrographs of hematoxylin and eosin-stained pancreas sections from mice treated with saline, cerulein, or cerulein + tricetin (TCT) (scale bar in the top row is 200  $\mu\text{m}$  and in the bottom row is 50  $\mu\text{m}$ ) (A). Micrographs of pancreas sections stained for TUNEL assay from the same three groups of mice (scale bar is 50  $\mu\text{m}$ ) (B). Edema, leukocyte infiltration, apoptosis (TUNEL assay), and necrosis scores (0–3) were determined by a pathologist (C). Error bars represent SD of six mice. Statistical analysis was performed with Fisher’s exact test. Stars (\*) indicate significant ( $p < 0.05$ ) differences between cerulein-treated and control groups. Hashtags (#) indicate significantly ( $p < 0.05$ ) reduced scores in the TCT group versus the cerulein-treated group.

### 3.7. Tricetin Suppresses Granulocyte Infiltration, Production of Inflammatory Mediators, and Synthesis of Poly(ADP-ribose) in Acute Pancreatitis

Tissue infiltration by white blood cells, especially granulocytes, is a hallmark of inflammation. Measuring tissue MPO levels is a good indicator of the granulocyte content of tissues. MPO activity increased close to sevenfold after induction of AP (Figure 6A). TCT treatment significantly reduced tissue MPO levels, suggesting suppression of granulocyte migration into the pancreas (Figure 6A).

The expression of IL1 $\beta$  and IL6 was upregulated in the pancreas in vivo (Figure 6B), similar to cerulein-treated isolated acinar cells. Pretreatment with TCT prevented the upregulation of IL1 $\beta$  and IL6 (Figure 6B). In contrast to the results in acinar cells, MMP2 levels did not change in vivo in the AP group and TCT did not affect MMP2 mRNA expression levels (Figure 6B). TNF $\alpha$ , an important mediator of AP in vivo [60] was not induced by cerulein in isolated acinar cells (Figure 2A). However, TNF $\alpha$  mRNA levels

increased in the pancreas after cerulein treatment, and TCT treatment significantly inhibited  $TNF\alpha$  expression (Figure 6B).

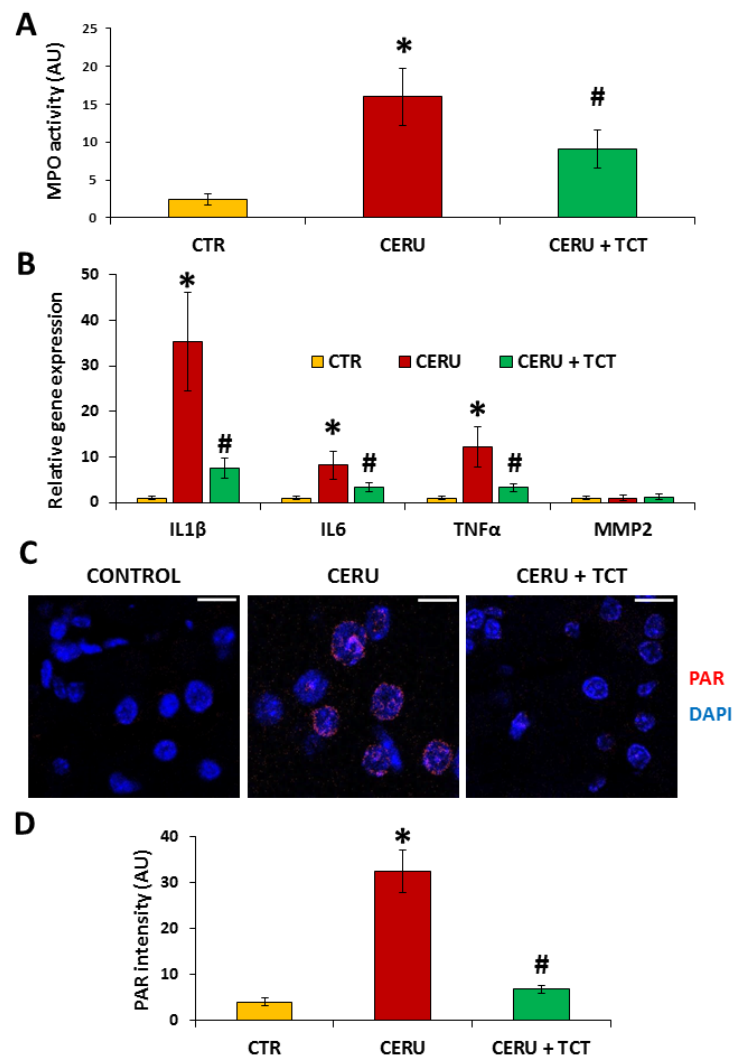


**Figure 6.** Tricetin inhibits inflammatory cell migration, PAR synthesis, and expression of inflammatory mediators in acute pancreatitis. Tricetin (TCT) treatment ( $2 \times 10$  mg/kg BW i.p.) suppressed neutrophil infiltration in the pancreas, as indicated by the decreased MPO level in the cerulein-induced acute pancreatitis model (A). TCT was effective in reducing IL1 $\beta$ , IL6, and TNF $\alpha$  expression, as indicated by the RT-qPCR assay data (B). Representative pictures of PAR immunofluorescent staining of pancreas sections are shown (C). The extent of PARylation was quantified by ImageJ software (D). TCT treatment ( $2 \times 10$  mg/kg BW i.p.) decreased PARylation in the cerulein-induced acute pancreatitis model (scale bar 20  $\mu$ m) (C,D). Error bars represent the SD of six mice. Statistical analysis was performed with one-way ANOVA test followed by Tukey's post hoc test. Stars (\*) indicate significant ( $p < 0.05$ ) differences between cerulein-treated and control groups. Hashtags (#) indicate significantly ( $p < 0.05$ ) reduced scores in the TCT group versus the cerulein-treated group.

PARP1 is a central mediator of inflammation and programmed necrotic cell death. We detected poly(ADP-ribose) (PAR) polymer, the product of PARP1, in tissue sections. A high number of nuclei in the exocrine pancreas were immunopositive for PAR (Figure 6C), indicating acinar PARP activation in AP. In contrast, PAR polymers were barely detectable in pancreas sections from TCT-treated animals (Figure 6C,D).

### 3.8. Posttreatment with Tricetin Protects Mice from Cerulein-Induced Acute Pancreatitis

The effects of TCT posttreatment on AP were examined (Figure 7A). TCT posttreatment significantly reduced acinar cell injury as reflected by decreased serum amylase and lipase levels (Figure 7B,C). Moreover, TCT significantly reduced pancreatic MPO levels, indicating suppression of granulocyte migration into the tissue (Figure 7D).

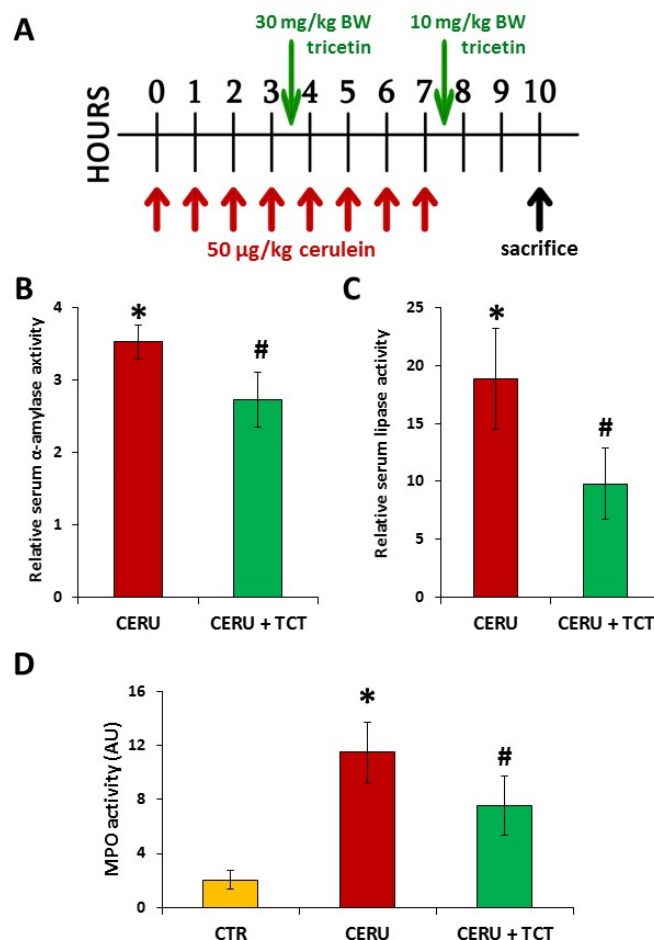


**Figure 7.** Posttreatment with tricetin inhibits tissue injury and inflammatory cell migration in acute pancreatitis. Acute pancreatitis was induced in mice with ( $8 \times 50 \mu\text{g/kg BW}$ , i.p.) cerulein treatment at hourly intervals. The animals were sacrificed 10 h after the first cerulein injection. Tricetin (TCT) was administered between the 4th and 5th cerulein injections ( $30 \text{ mg/kg BW}$ , i.p.) and after the last cerulein injection ( $10 \text{ mg/kg BW}$ ) (A). Serum levels of amylase and lipase were measured. Cerulein treatment significantly elevated serum  $\alpha$ -amylase and lipase levels. This elevation in serum  $\alpha$ -amylase and lipase levels was attenuated by TCT posttreatment (B,C). TCT suppressed neutrophil infiltration in the pancreas as indicated by the decreased tissue MPO levels (D). Error bars represent SD of six mice. Statistical analysis was performed with one-way ANOVA test followed by Tukey's post hoc test. Stars (\*) indicate significant ( $p < 0.05$ ) differences between cerulein-treated and control groups. Hashtags (#) indicate significantly ( $p < 0.05$ ) reduced values in the TCT group versus the cerulein-treated group.

## 4. Discussion

Despite intensive preclinical and clinical research, we still do not have an effective therapy for acute pancreatitis. While several flavonoids mitigate AP, the flavone compound TCT has not yet been studied. Our results showed that TCT prevented acinar cell injury and death and inflammation in both cell and animal models of AP.

To investigate the effects of TCT in AP, we chose cerulein exposure as a commonly used model displaying key events of AP both in primary acinar cell culture and in vivo. In

supraphysiologic concentrations, this cholecystokinin (CCK) analog peptide stimulates both CCK1 and CCK2 receptors. These G protein-coupled receptors trigger calcium signaling via PLC and inositol trisphosphate, resulting in reactive oxygen species (ROS) production, immune-inflammatory signaling (Jak/STAT, NF $\kappa$ B), and cell death [61]. Acinar cells also communicate with tissue macrophages *in vivo* to contribute to the pathogenesis of AP by inflammatory cytokine and chemokine production [62].

Cerulein triggered cell death in isolated primary murine acinar cells. Loss of cell viability in cerulein-treated acinar cells, as assessed by calcein assays, confirmed the toxic effects of CCK receptor overstimulation by cerulein. Moreover, cerulein-induced cell death had features of both apoptosis and necrosis, as indicated by caspase activation (apoptosis) as well as LDH release and propidium iodide uptake (indicators of necrosis). The significant cytoprotective effect of TCT could be observed both in the general viability assay as well as in apoptosis and necrosis assays. Moreover, TCT treatment helped maintain cellular viability in the mouse model of AP, as indicated by reduced serum amylase and lipase levels in TCT-treated animals compared with the serum levels in cerulein-treated mice. Interestingly, the effects of TCT were more pronounced on serum lipase activity than on amylase activity. This may be due to a more robust lipase release response compared to the less marked amylase release in the cerulein-treated animals. A previous study found that lipase is indeed a more sensitive indicator of pancreatitis [63]. Nevertheless, both serum markers confirmed the *in vivo* cytoprotective effects of TCT. TUNEL staining performed on pancreatic tissue sections also suggested that TCT prevents apoptotic cell death *in vivo*. The preserved pancreatic tissue architecture of TCT-treated animals also indicated less severe tissue injury in response to cerulein.

Since ROS production was implicated in cerulein-induced acinar cell injury and AP [64,65], we hypothesized that TCT may act, at least in part, by inhibiting ROS-induced cell death mediated by PARP1. Of note, the oxidative stress-induced and PARP1-mediated cell death pathway displays features of necrosis (including membrane permeabilization) [66], which are in line with the primarily necrotic nature of acinar cells in AP. Furthermore, some flavonoids have previously been shown to exert PARP inhibitory effects [67]. TCT inhibited PARP with a potency similar to 3-aminobenzamide. Moreover, in oxidatively-stressed primary pancreatic acinar cells, PAR polymer formation was observed, indicating PARP activation. TCT abolished PAR synthesis, as demonstrated in both immunofluorescent staining and Western blotting (Figure 3). Furthermore, in the cerulein-induced AP model, acinar cell nuclei contained PAR polymers, and TCT treatment abolished PAR formation (Figure 6). PARP1 and PARylation have been shown to contribute to the pathogenesis of AP [18,59]. Our current findings confirm that PARP inhibition by TCT translates to *in vivo* conditions, suggesting that PARP inhibition may be a key factor in the protection provided by TCT in AP. The cytoprotective effects of flavonoids might also be due to their effects on Akt signaling [68].

Oxidative stress is a common feature of various forms of inflammation, and it also plays a key role in the pathomechanism of AP. We hypothesized that an antioxidant mechanism may contribute to the protective effects of TCT in AP. Indeed, TCT had radical scavenging activity, as shown in the ABTS free radical capture assay. Interestingly, however, TCT did not protect against hydrogen peroxide-induced acinar cell injury (Supplementary Figure S2B–D). This may be due to the lack of hydrogen peroxide-specific antioxidant activity at the TCT concentration used in the assay. Moreover, instead of scavenging free radicals, antioxidants are known to act primarily by increasing the nucleophilic tone [69], inducing an antioxidant response via Nrf2 activation. Whether or not this is the case with TCT, requires further investigation.

Our data clearly indicate that TCT suppresses inflammation in AP. Reduced edema, suppressed inflammatory cell migration, and preserved tissue architecture support this statement (Figure 5). The underlying mechanism for the anti-inflammatory effects of TCT involves inhibition of the production of inflammatory mediators. From the cell-based experiments, we established that TCT inhibits the activation of inflammatory mediator

genes (Figure 2). Our *in vivo* data extended this list with  $\text{TNF}\alpha$  as a central mediator of inflammation induced by cerulein [70] and suppressed by TCT (Figure 6).  $\text{TNF}\alpha$  was not induced in acinar cell-based experiments, in line with our current understanding that macrophages are the main source of this cytokine in AP [71]. Thus, TCT may suppress inflammatory (cytokine, chemokine, MMP) gene activation both in acinar cells and in macrophages. We hypothesized that inhibition of  $\text{NF}\kappa\text{B}$  may be the underlying mechanism for this effect. Indeed, our data proved that TCT inhibits  $\text{NF}\kappa\text{B}$  activation in acinar cells (Figure 2B). It had no direct effect on the binding of the transcription factor to its consensus sequence (Figure 2C), suggesting that TCT interferes with a proximal step in the  $\text{NF}\kappa\text{B}$  signaling pathway. The effect of TCT on  $\text{NF}\kappa\text{B}$  may also be due to the PARP inhibitory effect of the drug, as PARP1 acts as a coactivator of  $\text{NF}\kappa\text{B}$  and PARP inhibition/PARP1 knockout suppresses  $\text{NF}\kappa\text{B}$  in a wide range of settings [58,72,73].

Although damage to acinar cells is the most studied cause of pancreatitis and the focus of our studies is also on these cells, we cannot ignore the fact that the disease is not only due to the failure of these cells. Early protease activation and  $\text{NF}\kappa\text{B}$  activation are essential features of AP; both occur in parallel during disease manifestation and strongly influence each other. However, not only protease and  $\text{NF}\kappa\text{B}$  activation play a critical role, but also the cell type in which their activation occurs is important [74].

Although the focus of this work was on the antioxidant and PARP inhibitory effect of TCT, it must be noted that TCT may also have additional effects contributing to its protection against pancreatitis. Pancreatic ischemia plays a dominant role in the development of AP, as well as in the progression of the disease into severe forms [75–77]. This statement is supported by observations that reduction in pancreatic blood flow increases the severity of acute pancreatitis [78], whereas improvement of pancreatic blood flow reduces the severity of acute pancreatitis and accelerates pancreatic recovery in this disease [79,80]. Previous studies have shown that the flavonoid quercetin [81,82] increased pancreatic blood flow in AP which translated into tissue protective effects and accelerated pancreatic recovery. Such observations suggest that the protective effect of tricetin on the pancreas in cerulein-induced AP may be, at least in part, related to the improvement of pancreatic blood flow.

## 5. Conclusions

In summary, TCT can be a novel candidate for the treatment of AP. TCT inhibits two central pathways of AP pathophysiology: acinar cell death and inflammation. The antioxidant and PARP inhibitory effects of TCT may play a central role in the protective effect of this flavone compound in AP.

**Supplementary Materials:** The following supporting information can be downloaded at: <https://www.mdpi.com/article/10.3390/biomedicines10061371/s1>, Figure S1: Low concentrations (1–30  $\mu\text{M}$ ) of tricetin are nontoxic to acinar cells; Figure S2: Tricetin did not affect hydrogen peroxide-induced acinar cell death.

**Author Contributions:** M.N.-P. and Z.H. planned and performed experiments, did statistical analysis, and wrote the manuscript; Z.R. planned and performed HCS analysis for PI assays and image analysis for Figures 3B,C and 6C,D; M.Á.D. and K.K. planned and performed experiments and evaluated data; T.E.-H. performed experiments; C.H. planned and performed experiments and evaluated data; J.M. and P.H. secured funding, designed experiments, and proofread the manuscript; L.V. obtained funding, designed and coordinated the study, and wrote the manuscript. All authors have read and agreed to the published version of the manuscript.

**Funding:** L.V. received funding from the National Research, Development and Innovation Office grants GINOP-2.3.2-15-2016-00020 TUMORDNS, GINOP-2.3.2-15-2016-00048-STAYALIVE, OTKA K132193, and K112336. C.H. received funding from the National Research, Development and Innovation Office grant PD 116845 and the Bolyai postdoctoral fellowship (BO/00468/17/8) and was supported by the ÚNKP-19-4-DE-299 New National Excellence Program of the Ministry of Human Capacities.

**Institutional Review Board Statement:** Animal experiments were approved by the institutional animal welfare committee of the University of Debrecen (25/2017/DEMÁB).

**Informed Consent Statement:** Not applicable.

**Data Availability Statement:** Data supporting reported results have been deposited in Zenodo ([doi:10.5281/zenodo.6526470](https://doi.org/10.5281/zenodo.6526470)).

**Acknowledgments:** The authors are grateful for the careful English language editing by Karen Uray.

**Conflicts of Interest:** The authors declare no conflict of interest. The funders had no role in the design of the study; in the collection, analyses, or interpretation of data; in the writing of the manuscript, or in the decision to publish the results.

## References

1. Czako, L.; Hegyi, P.; Rakonczay, Z., Jr.; Wittmann, T.; Otsuki, M. Interactions between the endocrine and exocrine pancreas and their clinical relevance. *Pancreatology* **2009**, *9*, 351–359. [[CrossRef](#)] [[PubMed](#)]
2. Hegyi, P.; Petersen, O.H. The exocrine pancreas: The acinar-ductal tango in physiology and pathophysiology. *Rev. Physiol. Biochem. Pharmacol.* **2013**, *165*, 1–30. [[CrossRef](#)] [[PubMed](#)]
3. Hegyi, P.; Maleth, J.; Venglovecz, V.; Rakonczay, Z., Jr. Pancreatic ductal bicarbonate secretion: Challenge of the acinar Acid load. *Front. Physiol.* **2011**, *2*, 36. [[CrossRef](#)] [[PubMed](#)]
4. Andralojc, K.M.; Mercalli, A.; Nowak, K.W.; Albarello, L.; Calcagno, R.; Luzi, L.; Bonifacio, E.; Doglioni, C.; Piemonti, L. Ghrelin-producing epsilon cells in the developing and adult human pancreas. *Diabetologia* **2009**, *52*, 486–493. [[CrossRef](#)]
5. Lutz, T.A. Creating the amylin story. *Appetite* **2022**, *172*, 105965. [[CrossRef](#)] [[PubMed](#)]
6. Parniczky, A.; Kui, B.; Szentesi, A.; Balazs, A.; Szucs, A.; Mosztbacher, D.; Czimmer, J.; Sarlos, P.; Bajor, J.; Godi, S.; et al. Prospective, Multicentre, Nationwide Clinical Data from 600 Cases of Acute Pancreatitis. *PLoS ONE* **2016**, *11*, e0165309. [[CrossRef](#)]
7. Meczker, A.; Hanak, L.; Parniczky, A.; Szentesi, A.; Eross, B.; Hegyi, P.; Hungarian Pancreatic Study Group. Analysis of 1060 Cases of Drug-Induced Acute Pancreatitis. *Gastroenterology* **2020**, *159*, 1958–1961.e8. [[CrossRef](#)] [[PubMed](#)]
8. Satoh, K.; Shimosegawa, T.; Masamune, A.; Hirota, M.; Kikuta, K.; Kihara, Y.; Kuriyama, S.; Tsuji, I.; Satoh, A.; Hamada, S.; et al. Nationwide epidemiological survey of acute pancreatitis in Japan. *Pancreas* **2011**, *40*, 503–507. [[CrossRef](#)]
9. Mosztbacher, D.; Hanak, L.; Farkas, N.; Szentesi, A.; Miko, A.; Bajor, J.; Sarlos, P.; Czimmer, J.; Vincze, A.; Hegyi, P.J.; et al. Hypertriglyceridemia-induced acute pancreatitis: A prospective, multicenter, international cohort analysis of 716 acute pancreatitis cases. *Pancreatology* **2020**, *20*, 608–616. [[CrossRef](#)]
10. Demcsak, A.; Soos, A.; Kincses, L.; Capunge, I.; Minkov, G.; Kovacheva-Slavova, M.; Nakov, R.; Wu, D.; Huang, W.; Xia, Q.; et al. Acid suppression therapy, gastrointestinal bleeding and infection in acute pancreatitis—An international cohort study. *Pancreatology* **2020**, *20*, 1323–1331. [[CrossRef](#)] [[PubMed](#)]
11. Parniczky, A.; Lantos, T.; Toth, E.M.; Szakacs, Z.; Godi, S.; Hagendorn, R.; Illes, D.; Koncz, B.; Marta, K.; Miko, A.; et al. Antibiotic therapy in acute pancreatitis: From global overuse to evidence based recommendations. *Pancreatology* **2019**, *19*, 488–499. [[CrossRef](#)] [[PubMed](#)]
12. Hritz, I.; Czako, L.; Dubravcsik, Z.; Farkas, G.; Kelemen, D.; Lasztity, N.; Morvay, Z.; Olah, A.; Pap, A.; Parniczky, A.; et al. Acute pancreatitis. Evidence-based practice guidelines, prepared by the Hungarian Pancreatic Study Group. *Orv. Hetil.* **2015**, *156*, 244–261. [[CrossRef](#)] [[PubMed](#)]
13. Marta, K.; Farkas, N.; Szabo, I.; Illes, A.; Vincze, A.; Par, G.; Sarlos, P.; Bajor, J.; Szucs, A.; Czimmer, J.; et al. Meta-Analysis of Early Nutrition: The Benefits of Enteral Feeding Compared to a Nil Per Os Diet Not Only in Severe, but Also in Mild and Moderate Acute Pancreatitis. *Int. J. Mol. Sci.* **2016**, *17*, 1691. [[CrossRef](#)]
14. Patai, A.; Solymosi, N.; Mohacsi, L.; Patai, A.V. Indomethacin and diclofenac in the prevention of post-ERCP pancreatitis: A systematic review and meta-analysis of prospective controlled trials. *Gastrointest. Endosc.* **2017**, *85*, 1144–1156.e1. [[CrossRef](#)]
15. Escobar, J.; Pereda, J.; Arduini, A.; Sandoval, J.; Moreno, M.L.; Perez, S.; Sabater, L.; Aparisi, L.; Cassinello, N.; Hidalgo, J.; et al. Oxidative and nitrosative stress in acute pancreatitis. Modulation by pentoxifylline and oxypurinol. *Biochem. Pharmacol.* **2012**, *83*, 122–130. [[CrossRef](#)]
16. Waldron, R.T.; Chen, Y.; Pham, H.; Go, A.; Su, H.Y.; Hu, C.; Wen, L.; Husain, S.Z.; Sugar, C.A.; Roos, J.; et al. The Orai Ca(2+) channel inhibitor CM4620 targets both parenchymal and immune cells to reduce inflammation in experimental acute pancreatitis. *J. Physiol.* **2019**, *597*, 3085–3105. [[CrossRef](#)]
17. Ahmad, A.; Haas De Mello, A.; Szczesny, B.; Toro, G.; Marcatti, M.; Druzhyina, N.; Liaudet, L.; Tarantini, S.; Salomao, R.; Garcia Soriano, F.; et al. Effects of the Poly(ADP-Ribose) Polymerase Inhibitor Olaparib in Cerulein-Induced Pancreatitis. *Shock* **2020**, *53*, 653–665. [[CrossRef](#)]
18. Mota, R.A.; Sanchez-Bueno, F.; Saenz, L.; Hernandez-Espinosa, D.; Jimeno, J.; Tornel, P.L.; Martinez-Torrano, A.; Ramirez, P.; Parrilla, P.; Yelamos, J. Inhibition of poly(ADP-ribose) polymerase attenuates the severity of acute pancreatitis and associated lung injury. *Lab. Invest.* **2005**, *85*, 1250–1262. [[CrossRef](#)]
19. Mabley, J.G.; Pacher, P.; Deb, A.; Wallace, R.; Elder, R.H.; Szabo, C. Potential role for 8-oxoguanine DNA glycosylase in regulating inflammation. *FASEB J.* **2005**, *19*, 290–292. [[CrossRef](#)]

20. Sandrasegaran, K.; Tahir, B.; Barad, U.; Fogel, E.; Akisik, F.; Tirkes, T.; Sherman, S. The Value of Secretin-Enhanced MRCP in Patients With Recurrent Acute Pancreatitis. *AJR Am. J. Roentgenol.* **2017**, *208*, 315–321. [[CrossRef](#)]
21. Wang, G.; Liu, Y.; Zhou, S.F.; Qiu, P.; Xu, L.; Wen, P.; Wen, J.; Xiao, X. Effect of Somatostatin, Ulinastatin and Gabexate on the Treatment of Severe Acute Pancreatitis. *Am. J. Med. Sci.* **2016**, *351*, 506–512. [[CrossRef](#)] [[PubMed](#)]
22. Nakamichi, I.; Habtezion, A.; Zhong, B.; Contag, C.H.; Butcher, E.C.; Omary, M.B. Hemin-activated macrophages home to the pancreas and protect from acute pancreatitis via heme oxygenase-1 induction. *J. Clin. Investig.* **2005**, *115*, 3007–3014. [[CrossRef](#)] [[PubMed](#)]
23. Schneider, L.; Jabrailova, B.; Soliman, H.; Hofer, S.; Strobel, O.; Hackert, T.; Buchler, M.W.; Werner, J. Pharmacological cholinergic stimulation as a therapeutic tool in experimental necrotizing pancreatitis. *Pancreas* **2014**, *43*, 41–46. [[CrossRef](#)]
24. Tekin, S.O.; Teksoz, S.; Terzioğlu, D.; Arikan, A.E.; Ozcevik, H.; Uslu, E. Use of infliximab in treatment of acute pancreatitis. *Bratisl. Lek. Listy* **2015**, *116*, 167–172. [[CrossRef](#)]
25. Abu-El-Haija, M.; Gukovskaya, A.S.; Andersen, D.K.; Gardner, T.B.; Hegyi, P.; Pandol, S.J.; Papachristou, G.I.; Saluja, A.K.; Singh, V.K.; Uc, A.; et al. Accelerating the Drug Delivery Pipeline for Acute and Chronic Pancreatitis: Summary of the Working Group on Drug Development and Trials in Acute Pancreatitis at the National Institute of Diabetes and Digestive and Kidney Diseases Workshop. *Pancreas* **2018**, *47*, 1185–1192. [[CrossRef](#)]
26. Bakondi, E.; Singh, S.B.; Hajnady, Z.; Nagy-Penzes, M.; Regdon, Z.; Kovacs, K.; Hegedus, C.; Madacsy, T.; Maleth, J.; Hegyi, P.; et al. Spilanthal Inhibits Inflammatory Transcription Factors and iNOS Expression in Macrophages and Exerts Anti-inflammatory Effects in Dermatitis and Pancreatitis. *Int. J. Mol. Sci.* **2019**, *20*, 4308. [[CrossRef](#)]
27. Foitzik, T.; Stuffer, M.; Hotz, H.G.; Klinnert, J.; Wagner, J.; Warshaw, A.L.; Schulzke, J.D.; Fromm, M.; Buhr, H.J. Glutamine stabilizes intestinal permeability and reduces pancreatic infection in acute experimental pancreatitis. *J. Gastrointest. Surg.* **1997**, *1*, 40–46. [[CrossRef](#)]
28. Kim, N.; Park, J.M.; Lee, S.H.; Kim, B.H.; Son, J.H.; Ryu, J.K.; Kim, Y.T.; Lee, W. Effect of Combinatory Treatment with Resveratrol and Guggulsterone on Mild Acute Pancreatitis in Mice. *Pancreas* **2017**, *46*, 366–371. [[CrossRef](#)]
29. Tsang, S.W.; Guan, Y.F.; Wang, J.; Bian, Z.X.; Zhang, H.J. Inhibition of pancreatic oxidative damage by stilbene derivative dihydro-resveratrol: Implication for treatment of acute pancreatitis. *Sci. Rep.* **2016**, *6*, 22859. [[CrossRef](#)]
30. Gasic, U.; Ciric, I.; Pejic, T.; Radenkovic, D.; Djordjevic, V.; Radulovic, S.; Tesic, Z. Polyphenols as Possible Agents for Pancreatic Diseases. *Antioxidants* **2020**, *9*, 547. [[CrossRef](#)]
31. Xia, S.; Wang, J.; Kalionis, B.; Zhang, W.; Zhao, Y. Genistein protects against acute pancreatitis via activation of an apoptotic pathway mediated through endoplasmic reticulum stress in rats. *Biochem. Biophys. Res. Commun.* **2019**, *509*, 421–428. [[CrossRef](#)] [[PubMed](#)]
32. Sheng, B.; Zhao, L.; Zang, X.; Zhen, J.; Liu, Y.; Bian, W.; Chen, W. Quercetin inhibits caerulein-induced acute pancreatitis through regulating miR-216b by targeting MAP2K6 and NEAT1. *Inflammopharmacology* **2021**, *29*, 549–559. [[CrossRef](#)]
33. Li, Y.; Pan, Y.; Gao, L.; Zhang, J.; Xie, X.; Tong, Z.; Li, B.; Li, G.; Lu, G.; Li, W. Naringenin Protects against Acute Pancreatitis in Two Experimental Models in Mice by NLRP3 and Nrf2/HO-1 Pathways. *Mediators Inflamm.* **2018**, *2018*, 3232491. [[CrossRef](#)] [[PubMed](#)]
34. Mrazek, A.A.; Bhatia, V.; Falzon, M.; Spratt, H.; Chao, C.; Hellmich, M.R. Apigenin Decreases Acinar Cell Damage in Pancreatitis. *Pancreas* **2019**, *48*, 711–718. [[CrossRef](#)]
35. Jia, R.; Ma, J.; Meng, W.; Wang, N. Dihydromyricetin inhibits caerulein-induced TRAF3-p38 signaling activation and acute pancreatitis response. *Biochem. Biophys. Res. Commun.* **2018**, *503*, 1696–1702. [[CrossRef](#)] [[PubMed](#)]
36. Xiong, J.; Wang, K.; Yuan, C.; Xing, R.; Ni, J.; Hu, G.; Chen, F.; Wang, X. Luteolin protects mice from severe acute pancreatitis by exerting HO-1-mediated anti-inflammatory and antioxidant effects. *Int. J. Mol. Med.* **2017**, *39*, 113–125. [[CrossRef](#)] [[PubMed](#)]
37. Jo, I.J.; Bae, G.S.; Choi, S.B.; Kim, D.G.; Shin, J.Y.; Seo, S.H.; Choi, M.O.; Kim, T.H.; Song, H.J.; Park, S.J. Fisetin attenuates cerulein-induced acute pancreatitis through down regulation of JNK and NF-kappaB signaling pathways. *Eur. J. Pharmacol.* **2014**, *737*, 149–158. [[CrossRef](#)]
38. Gaman, L.; Dragos, D.; Vlad, A.; Robu, G.C.; Radoi, M.P.; Stroica, L.; Badea, M.; Gilca, M. Phytochemicals in Acute Pancreatitis: Targeting the Balance between Apoptosis and Necrosis. *Evid.-Based Complement. Altern. Med.* **2018**, *2018*, 5264592. [[CrossRef](#)]
39. Shapiro, H.; Singer, P.; Halpern, Z.; Bruck, R. Polyphenols in the treatment of inflammatory bowel disease and acute pancreatitis. *Gut* **2007**, *56*, 426–435. [[CrossRef](#)]
40. Ren, J.; Yuan, L.; Wang, W.; Zhang, M.; Wang, Q.; Li, S.; Zhang, L.; Hu, K. Tricetin protects against 6-OHDA-induced neurotoxicity in Parkinson's disease model by activating Nrf2/HO-1 signaling pathway and preventing mitochondria-dependent apoptosis pathway. *Toxicol. Appl. Pharmacol.* **2019**, *378*, 114617. [[CrossRef](#)]
41. Ge, Q.; Chen, L.; Tang, M.; Zhang, S.; Liu, L.; Gao, L.; Ma, S.; Kong, M.; Yao, Q.; Feng, F.; et al. Analysis of mulberry leaf components in the treatment of diabetes using network pharmacology. *Eur. J. Pharmacol.* **2018**, *833*, 50–62. [[CrossRef](#)] [[PubMed](#)]
42. Wang, N.; Zhu, F.; Shen, M.; Qiu, L.; Tang, M.; Xia, H.; Chen, L.; Yuan, Y.; Ma, S.; Chen, K. Network pharmacology-based analysis on bioactive anti-diabetic compounds in *Potentilla discolor bunge*. *J. Ethnopharmacol.* **2019**, *241*, 111905. [[CrossRef](#)] [[PubMed](#)]
43. Pistelli, L.; Bertoli, A.; Nocchioli, C.; Mendez, J.; Musmanno, R.A.; Di Maggio, T.; Coratza, G. Antimicrobial activity of *Inga fenderiana* extracts and isolated flavonoids. *Nat. Prod. Commun.* **2009**, *4*, 1679–1683. [[CrossRef](#)] [[PubMed](#)]
44. Chang, P.Y.; Hsieh, M.J.; Hsieh, Y.S.; Chen, P.N.; Yang, J.S.; Lo, F.C.; Yang, S.F.; Lu, K.H. Tricetin inhibits human osteosarcoma cells metastasis by transcriptionally repressing MMP-9 via p38 and Akt pathways. *Environ. Toxicol.* **2017**, *32*, 2032–2040. [[CrossRef](#)] [[PubMed](#)]

45. Chao, R.; Chow, J.M.; Hsieh, Y.H.; Chen, C.K.; Lee, W.J.; Hsieh, F.K.; Yu, N.Y.; Chou, M.C.; Cheng, C.W.; Yang, S.F.; et al. Tricetin suppresses the migration/invasion of human glioblastoma multiforme cells by inhibiting matrix metalloproteinase-2 through modulation of the expression and transcriptional activity of specificity protein 1. *Expert Opin. Ther. Targets* **2015**, *19*, 1293–1306. [[CrossRef](#)] [[PubMed](#)]
46. Hung, J.Y.; Chang, W.A.; Tsai, Y.M.; Hsu, Y.L.; Chiang, H.H.; Chou, S.H.; Huang, M.S.; Kuo, P.L. Tricetin, a dietary flavonoid, suppresses benzo(a)pyrene-induced human nonsmall cell lung cancer bone metastasis. *Int. J. Oncol.* **2015**, *46*, 1985–1993. [[CrossRef](#)] [[PubMed](#)]
47. Cai, L.; Zhang, X.; Hou, M.; Gao, F. Natural flavone tricetin suppresses oxidized LDL-induced endothelial inflammation mediated by Egr-1. *Int. Immunopharmacol.* **2020**, *80*, 106224. [[CrossRef](#)] [[PubMed](#)]
48. Sun, F.F.; Hu, P.F.; Xiong, Y.; Bao, J.P.; Qian, J.; Wu, L.D. Tricetin Protects Rat Chondrocytes against IL-1 $\beta$ -Induced Inflammation and Apoptosis. *Oxid. Med. Cell Longev.* **2019**, *2019*, 4695381. [[CrossRef](#)] [[PubMed](#)]
49. Wang, X.; Wang, Z.; Sidhu, P.S.; Desai, U.R.; Zhou, Q. 6-Hydroxyflavone and derivatives exhibit potent anti-inflammatory activity among mono-, di- and polyhydroxylated flavones in kidney mesangial cells. *PLoS ONE* **2015**, *10*, e0116409. [[CrossRef](#)] [[PubMed](#)]
50. Gout, J.; Pommier, R.M.; Vincent, D.F.; Kaniewski, B.; Martel, S.; Valcourt, U.; Bartholin, L. Isolation and culture of mouse primary pancreatic acinar cells. *J. Vis. Exp.* **2013**, *78*, 50514. [[CrossRef](#)]
51. Hegedus, C.; Lakatos, P.; Kiss-Szikszai, A.; Patonay, T.; Gergely, S.; Gregus, A.; Bai, P.; Hasko, G.; Szabo, E.; Virag, L. Cytoprotective dibenzoylmethane derivatives protect cells from oxidative stress-induced necrotic cell death. *Pharmacol. Res.* **2013**, *72*, 25–34. [[CrossRef](#)] [[PubMed](#)]
52. Regdon, Z.; Robaszekiewicz, A.; Kovacs, K.; Rygielska, Z.; Hegedus, C.; Bodoor, K.; Szabo, E.; Virag, L. LPS protects macrophages from AIF-independent parthanatos by downregulation of PARP1 expression, induction of SOD2 expression, and a metabolic shift to aerobic glycolysis. *Free Radic. Biol. Med.* **2019**, *131*, 184–196. [[CrossRef](#)]
53. Hegyi, P.; Venglovecz, V.; Pallagi, P.; Maleth, J.; Takacs, T.; Rakonczay, Z., Jr. Galanin, a potent inhibitor of pancreatic bicarbonate secretion, is involved in the induction and progression of cerulein-induced experimental acute pancreatitis. *Pancreas* **2011**, *40*, 155–156, author reply 156–157. [[CrossRef](#)]
54. Kim, D.U.; Bae, G.S.; Kim, M.J.; Choi, J.W.; Kim, D.G.; Song, H.J.; Park, S.J. Icaritin attenuates the severity of cerulein-induced acute pancreatitis by inhibiting p38 activation in mice. *Int. J. Mol. Med.* **2019**, *44*, 1563–1573. [[CrossRef](#)]
55. Kiernan, J.A. *Histological and Histochemical Methods: Theory and Practice*, 5th ed.; Scion Publishing: Banbury, UK, 2015; pp. 454–490.
56. Ceranowicz, P.; Warzecha, Z.; Dembinski, A.; Cieszkowski, J.; Dembinski, M.; Sendur, R.; Kusnierz-Cabala, B.; Tomaszewska, R.; Kuwahara, A.; Kato, I. Pretreatment with obestatin inhibits the development of cerulein-induced pancreatitis. *J. Physiol. Pharmacol.* **2009**, *60*, 95–101. [[PubMed](#)]
57. Regdon, Z.; Demeny, M.A.; Kovacs, K.; Hajnady, Z.; Nagy-Penzes, M.; Bakondi, E.; Kiss, A.; Hegedus, C.; Virag, L. High-content screening identifies inhibitors of oxidative stress-induced parthanatos: Cytoprotective and anti-inflammatory effects of ciclopirox. *Br. J. Pharmacol.* **2021**, *178*, 1095–1113. [[CrossRef](#)]
58. El-Hamoly, T.; Hajnady, Z.; Nagy-Penzes, M.; Bakondi, E.; Regdon, Z.; Demeny, M.A.; Kovacs, K.; Hegedus, C.; Abd El-Rahman, S.S.; Szabo, E.; et al. Poly(ADP-Ribose) Polymerase 1 Promotes Inflammation and Fibrosis in a Mouse Model of Chronic Pancreatitis. *Int. J. Mol. Sci.* **2021**, *22*, 3593. [[CrossRef](#)]
59. Martinez-Bosch, N.; Fernandez-Zapico, M.E.; Navarro, P.; Yelamos, J. Poly(ADP-Ribose) Polymerases: New Players in the Pathogenesis of Exocrine Pancreatic Diseases. *Am. J. Pathol.* **2016**, *186*, 234–241. [[CrossRef](#)]
60. Tasci, S.; Senocak, R.; Lapsekili, E.; Kaymak, S.; Yigit, T. The effects of a TNF- $\alpha$  inhibitor and HBO combination on the severity of pancreatitis and oxidative response in an experimental model of acute pancreatitis. *Bratisl. Lek. Listy* **2019**, *120*, 417–422. [[CrossRef](#)]
61. Kim, H. Cerulein pancreatitis: Oxidative stress, inflammation, and apoptosis. *Gut Liver* **2008**, *2*, 74–80. [[CrossRef](#)] [[PubMed](#)]
62. Zhao, Y.; Wang, H.; Lu, M.; Qiao, X.; Sun, B.; Zhang, W.; Xue, D. Pancreatic Acinar Cells Employ miRNAs as Mediators of Intercellular Communication to Participate in the Regulation of Pancreatitis-Associated Macrophage Activation. *Mediat. Inflamm.* **2016**, *2016*, 6340457. [[CrossRef](#)]
63. Gwozdz, G.P.; Steinberg, W.M.; Werner, M.; Henry, J.P.; Pauley, C. Comparative evaluation of the diagnosis of acute pancreatitis based on serum and urine enzyme assays. *Clin. Chim. Acta* **1990**, *187*, 243–254. [[CrossRef](#)]
64. Dabrowski, A.; Konturek, S.J.; Konturek, J.W.; Gabryelewicz, A. Role of oxidative stress in the pathogenesis of caerulein-induced acute pancreatitis. *Eur. J. Pharmacol.* **1999**, *377*, 1–11. [[CrossRef](#)]
65. Yu, J.H.; Kim, H. Oxidative stress and inflammatory signaling in cerulein pancreatitis. *World J. Gastroenterol.* **2014**, *20*, 17324–17329. [[CrossRef](#)] [[PubMed](#)]
66. Virag, L.; Robaszekiewicz, A.; Rodriguez-Vargas, J.M.; Oliver, F.J. Poly(ADP-ribose) signaling in cell death. *Mol. Asp. Med.* **2013**, *34*, 1153–1167. [[CrossRef](#)]
67. Geraets, L.; Moonen, H.J.; Brauers, K.; Wouters, E.F.; Bast, A.; Hageman, G.J. Dietary flavones and flavonoles are inhibitors of poly(ADP-ribose)polymerase-1 in pulmonary epithelial cells. *J. Nutr.* **2007**, *137*, 2190–2195. [[CrossRef](#)]
68. Williams, R.J.; Spencer, J.P.; Rice-Evans, C. Flavonoids: Antioxidants or signalling molecules? *Free Radic. Biol. Med.* **2004**, *36*, 838–849. [[CrossRef](#)] [[PubMed](#)]
69. Forman, H.J.; Davies, K.J.; Ursini, F. How do nutritional antioxidants really work: Nucleophilic tone and para-hormesis versus free radical scavenging in vivo. *Free Radic. Biol. Med.* **2014**, *66*, 24–35. [[CrossRef](#)]

70. Malleo, G.; Mazzon, E.; Siriwardena, A.K.; Cuzzocrea, S. Role of tumor necrosis factor-alpha in acute pancreatitis: From biological basis to clinical evidence. *Shock* **2007**, *28*, 130–140. [[CrossRef](#)] [[PubMed](#)]
71. Gea-Sorli, S.; Closa, D. Role of macrophages in the progression of acute pancreatitis. *World J. Gastrointest. Pharmacol. Ther.* **2010**, *1*, 107–111. [[CrossRef](#)] [[PubMed](#)]
72. Bai, P.; Virag, L. Role of poly(ADP-ribose) polymerases in the regulation of inflammatory processes. *FEBS Lett.* **2012**, *586*, 3771–3777. [[CrossRef](#)]
73. Demeny, M.A.; Virag, L. The PARP Enzyme Family and the Hallmarks of Cancer Part 2: Hallmarks Related to Cancer Host Interactions. *Cancers* **2021**, *13*, 2057. [[CrossRef](#)]
74. Mayerle, J.; Sandler, M.; Hegyi, E.; Beyer, G.; Lerch, M.M.; Sahin-Toth, M. Genetics, Cell Biology, and Pathophysiology of Pancreatitis. *Gastroenterology* **2019**, *156*, 1951–1968 e1951. [[CrossRef](#)]
75. Gullo, L.; Cavicchi, L.; Tomassetti, P.; Spagnolo, C.; Freyrie, A.; D’Addato, M. Effects of ischemia on the human pancreas. *Gastroenterology* **1996**, *111*, 1033–1038. [[CrossRef](#)]
76. Lonardo, A.; Grisendi, A.; Bonilauri, S.; Rambaldi, M.; Selmi, I.; Tondelli, E. Ischaemic necrotizing pancreatitis after cardiac surgery. A case report and review of the literature. *Ital. J. Gastroenterol. Hepatol.* **1999**, *31*, 872–875.
77. Dembinski, A.; Warzecha, Z.; Ceranowicz, P.; Stachura, J.; Tomaszewska, R.; Konturek, S.J.; Sendur, R.; Dembinski, M.; Pawlik, W.W. Pancreatic damage and regeneration in the course of ischemia-reperfusion induced pancreatitis in rats. *J. Physiol. Pharmacol.* **2001**, *52*, 221–235.
78. Furukawa, M.; Kimura, T.; Sumii, T.; Yamaguchi, H.; Nawata, H. Role of local pancreatic blood flow in development of hemorrhagic pancreatitis induced by stress in rats. *Pancreas* **1993**, *8*, 499–505. [[CrossRef](#)]
79. Warzecha, Z.; Dembinski, A.; Ceranowicz, P.; Dembinski, M.; Cieszkowski, J.; Kusnierz-Cabala, B.; Naskalski, J.W.; Jaworek, J.; Konturek, S.J.; Pawlik, W.W.; et al. Influence of ischemic preconditioning on blood coagulation, fibrinolytic activity and pancreatic repair in the course of caerulein-induced acute pancreatitis in rats. *J. Physiol. Pharmacol.* **2007**, *58*, 303–319. [[PubMed](#)]
80. Maduzia, D.; Ceranowicz, P.; Cieszkowski, J.; Chmura, A.; Galazka, K.; Kusnierz-Cabala, B.; Warzecha, Z. Administration of warfarin accelerates the recovery in ischemia/reperfusion-induced acute pancreatitis. *J. Physiol. Pharmacol.* **2020**, *71*, 417–427. [[CrossRef](#)]
81. Vovkun, T.V.; Yanchuk, P.I.; Shtanova, L.Y.; Shalamay, A.S. Tissue Blood Flow in the Digestive Organs of Rats with Acute Pancreatitis after Corvutin Administration. *Fiziol. Zhurnal* **2015**, *61*, 53–59. [[CrossRef](#)]
82. Datsyuk, O.I. Impact of Quercetin on Systemic and Splanchnic Blood Circulation in a Complex of Preoperative Preparation in Patients, Suffering an Acute Pancreatitis. *Klin Khir* **2016**, 13–15. [[PubMed](#)]